



Article

# Aurophilic Interactions of Dimeric Bisphosphine Gold(I) Complexes Pre-Organized by the Structure of the 1,5-Diaza-3,7-Diphosphacyclooctanes

Irina R. Dayanova <sup>1</sup>, Adelina I. Favezova <sup>1</sup>, Igor D. Strelnik <sup>1</sup>, Igor A. Litvinov <sup>1</sup>, Daut R. Islamov <sup>1</sup>, Ilya E. Kolesnikov <sup>2</sup>, Tatiana P. Gerasimova <sup>1,\*</sup> and Andrey A. Karasik <sup>1</sup>

<sup>1</sup> Arbuzov Institute of Organic and Physical Chemistry, FRC Kazan Scientific Center, Russian Academy of Sciences, 8 Arbuzov Street, 420088 Kazan, Russia

<sup>2</sup> Center for Optical and Laser Materials Research, Saint Petersburg State University, 7/9 Universitetskaya nab., 1990345 St. Petersburg, Russia

\* Correspondence: elli@iopc.ru



**Citation:** Dayanova, I.R.; Favezova, A.I.; Strelnik, I.D.; Litvinov, I.A.; Islamov, D.R.; Kolesnikov, I.E.; Gerasimova, T.P.; Musina, E.I.; Karasik, A.A. Aurophilic Interactions of Dimeric Bisphosphine Gold(I) Complexes Pre-Organized by the Structure of the 1,5-Diaza-3,7-Diphosphacyclooctanes. *Inorganics* **2022**, *10*, 224. <https://doi.org/10.3390/inorganics10120224>

Academic Editor: Alexander Artem'ev

Received: 26 October 2022

Accepted: 22 November 2022

Published: 25 November 2022

**Publisher's Note:** MDPI stays neutral with regard to jurisdictional claims in published maps and institutional affiliations.



**Copyright:** © 2022 by the authors. Licensee MDPI, Basel, Switzerland. This article is an open access article distributed under the terms and conditions of the Creative Commons Attribution (CC BY) license (<https://creativecommons.org/licenses/by/4.0/>).

**Abstract:** The dimeric gold(I) chloride and gold(I) iodide complexes ( $[L_2Au]Cl_2$  and  $L_2AuI_2$ ) on the scaffold of the cyclic bisphosphine, namely 1,5-diaza-3,7-diphosphacyclooctane containing  $\alpha$ -phenylbenzyl (benzhydryl) substituents at the nitrogen atoms, were synthesized. The obtained complexes were isolated as white crystalline powders. The single crystal XRD of the obtained complexes revealed the strong aurophilic interactions between two gold(I) atoms with the  $Au \cdots Au$  distance values of 2.9977(6) and 3.1680(5) Å. The comparison of the gold complexes, based on the *N,N*-diaryl- and *N,N*-dibenzhydryl substituted 1,5-diaza-3,7-diphosphacyclooctanes, allowed to reveal the strong impact of the initial heterocycle conformation on the realization of the aurophilic interactions, where the geometry of *N,N*-dibenzhydryl substituted 1,5-diaza-3,7-diphosphacyclooctane, is pre-organized for the intramolecular aurophilic interactions of the complexes. The obtained complexes exhibit a bluish-green phosphorescence ( $\lambda_{em}$  505 (-Cl) and 530(-I)) in the solid state at room temperature, originated by the metal-halide centered transitions, which was confirmed by the TDDFT calculations. It was found that the aurophilic interactions are realized in the ground and in the triplet excited states of the complexes. The slighter change of the geometry of the *N,N*-dibenzhydryl substituted gold(I) iodide complexes, under the transition from the ground state to the excited state, in comparison with their *N,N*-diaryl substituted analogues, results in the reduced values of the Stokes shift of luminescence (ca. 150 nm vs. 175 nm).

**Keywords:** gold(I) complexes; luminescence; d10-complexes; aminomethylphosphines; bisphosphines

## 1. Introduction

Aurophilic interactions are an attractive phenomenon actively studied in the terms of gold(I) complexes exhibiting intriguing photophysical properties [1–5]. Various bidentate P-, S- or (NHC)-ligands are often applied for the design of flexible dinuclear gold(I) complexes, where the intramolecular aurophilic interactions can switch, depending on the external factors [6–12]. This phenomenon produces various ways for the stimuli-responsive luminescence in a solid state and in solutions, such as the vapochromism, solvatochromism, mechanochromism and the thermochromism of luminescence [2,13–17]. Due to rich photophysical properties and the dependence of luminescence on the external factors, gold(I) complexes become perspective precursors for the design of the optical materials with possible applications in medicine and technology [18–20].

Dimeric gold(I) complexes ( $[(L-L)_2Au_2]$ ), based on the bidentate phosphine ligands are able to form intramolecular interactions in the ground and excited states, affecting on their luminescence [1,21–24]. The flexibility of the ligands' backbone provides the formation of the  $Au \cdots Au$  interactions in the excited states and, consequently, induces the triplet

metal-halide centered ( $^3(M+X)C$ ) emission of the complexes. Typically, the intraligand triplet state of such complexes lies at a higher energy than the metal-halide centered triplet excited state, originated from the Au  $\cdots$  Au interactions [22,25]. The aurophilic interaction in the excited states can be realized even in the complexes displaying a quite large distance between two gold(I) ions in the ground states [6,22,26]. Recently, such a  $^3(M+X)C$  state emission was established for the dinuclear gold(I) complexes of *N,N*-diaryl substituted 1,5-diaza-3,7-diphosphacyclooctanes [26–28]. The intramolecular Au  $\cdots$  Au distance of these complexes in the ground states is ca. 5 Å, whereas in the lowest triplet excited states, this value decreases to ca. 2.9 Å, which is less than the sum of the van der Waals radii of gold(I) ions [28]. We supposed that the conformational flexibility of the cyclic bisphosphine backbone is responsible for the shortening and elongating of the distances between two gold(I) ions in these complexes.

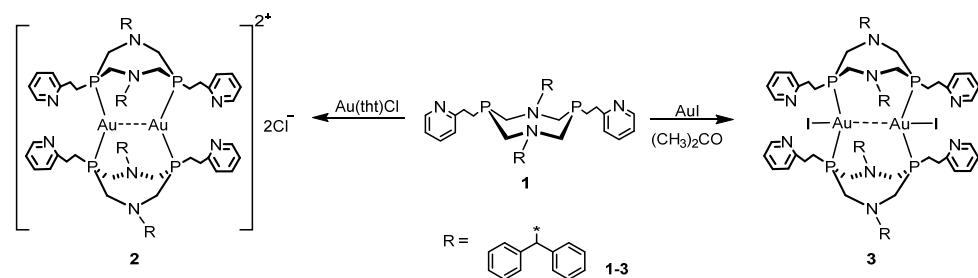
Recently we demonstrated the different coordination behavior of *N,N*-diaryl- and *N,N*-dibenzyl substituted 1,5-diaza-3,7-diphosphacyclooctanes, relative to copper(I) iodide, which was probably caused by the different mutual orientations of the two phosphorus lone pairs in the initial ligands [29]. So, the phosphorus lone pairs of *N,N*-dibenzyl substituted 1,5-diaza-3,7-diphosphacyclooctanes are directed toward each other and are preorganized for the chelate binding [30], whereas the phosphorus lone pairs of *N*-aryl substituted 1,5-diaza-3,7-diphosphacyclooctanes [31], are oriented in nearly a parallel manner and are preorganized for the bridge coordination mode of the diphosphine ligand.

Therefore, recent findings opened a question regarding the coordination behavior of *N,N*-dibenzyl substituted 1,5-diaza-3,7-diphosphacyclooctanes relative to the gold(I) ion.

In the present work, we utilized *N,N*-bis( $\alpha$ -phenylbenzyl) substituted 1,5-diaza-3,7-diphosphacyclooctanes for the synthesis of dimeric gold(I) complexes with the aim to reveal the role of the substituents in the nitrogen atoms of diazdiphosphacyclooctanes for the lability and photophysical properties of their dimeric gold(I) complexes.

## 2. Results and Discussion

*Synthesis and structure.* The initial ligand **1** was obtained, according the common procedures for the synthesis of 1,5-diaza-3,7-diphosphacyclooctanes [30,32,33]. The reaction of ligand **1** with Au(tht)Cl or AuI in a 1:1 ratio in acetone, resulted in the formation of complexes **2** and **3** (Scheme 1).



**Scheme 1.** The synthesis of complexes **2** and **3**.

The  $^1H$  NMR and  $^{31}P$  spectra confirm the coordination of the phosphorus atoms to the gold(I) ions. In the  $^{31}P\{^1H\}$  NMR spectra of the complexes, one broad singlet at ca. 27–31 ppm is observed, whereas one set of signals in the  $^1H$  NMR spectra of **2** and **3** indicates the formation of the single compounds. The ESI mass spectra of the complexes display the peak at  $m/z$  889, corresponding to the  $[Au_2L_2]^{2+}$  ion of **2** and **3** and the peak with  $m/z$  1905, corresponding to the  $[Au_2L_2I]^+$  ion of **3**.

The structures of complexes **2** and **3** were unambiguously confirmed by the XRD analysis. Crystals of complex **2** were obtained at room temperature by the slow diffusion of dibutyl ether into a solution of the complex in dichloromethane, whereas crystals of complex **3** were obtained by the recrystallization from dimethylformamide (Figures 1, S1 and S2).

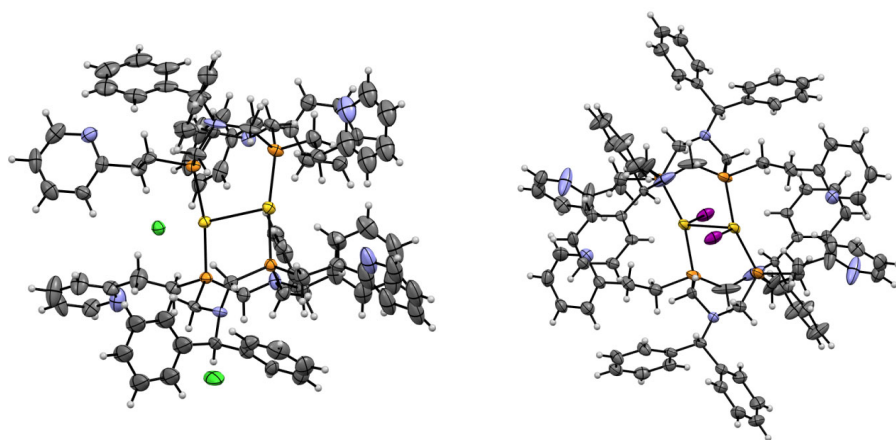


**Figure 1.** Molecular structure of complexes **2** and **3**. Selected interatomic distances are presented in Table S1.

The crystals of both complexes contain two independent molecules in the unit cell (Table 1).

**Table 1.** Selected crystallographic characteristics of complexes **2** and **3**.

Compound	2	3
Moiety Formula	$C_{88}H_{92}Au_2N_8P_4$ , $CH_2Cl_2$ , 2(Cl) [+ solvent]	$C_{88}H_{92}Au_2I_2N_8P_4$
Formula	$C_{88}H_{94}Au_2Cl_2N_8P_4$	$C_{88}H_{92}Au_2I_2N_8P_4$
Formula Weight	1935.35	2033.30
Crystal System	triclinic	triclinic
Space Group	P-1 (P1bar)	P-1 (P1bar)
Temp. of Measurement, K	110(2)	100(2)
Cell Parameters	$a = 20.3117(19) \text{ \AA}$ $b = 21.479(2) \text{ \AA}$ $c = 23.204(2) \text{ \AA}$ $\alpha = 109.568(3)^\circ$ $\beta = 105.798(3)^\circ$ $\gamma = 103.892(3)^\circ$	$a = 15.7816(3) \text{ \AA}$ $b = 16.8956(4) \text{ \AA}$ $c = 17.5198(4) \text{ \AA}$ $\alpha = 73.294(2)^\circ$ $\beta = 67.489(2)^\circ$ $\gamma = 84.5748(17)^\circ$
$V [\text{\AA}^3]$	8543.7(14)	4132.75(17)
Z and $Z'$	<b>2 and 1</b> <b>4 and 2</b>	Two independent molecules in the special position in the centers of symmetry
$D(\text{calc}) [\text{g/cm}^3]$	1.505	1.634
$\lambda (\text{\AA})$	(MoK $\alpha$ ) 0.71073	(CuK $\alpha$ ) 1.54184
$\mu [\text{mm}^{-1}]$	3.679	13.554
F(000)	3880	2000
Theta Min-Max [Deg]	1.8–26.5°	2.7–76.7°
Reflections Measured	310,069	55,670
Independent Reflections	35,148	16,836
Observed Reflections [ $I > 2\sigma(I)$ ]	23,952	15,034
Goodness of Fit	1.065	1.090

**Table 1.** Cont.

Compound	2	3
R [I > 2σ(I)]	R1 = 0.0677, wR2 = 0.1564	R1 = 0.0394, wR2 = 0.1040
R (all reflections)	R1 = 0.1098, wR2 = 0.1766	R1 = 0.0454, wR2 = 0.1071
Max. and Min. Resd. Dens. [e/Å <sup>-3</sup> ]	3.140 and -2.185	2.04 and -1.28
Deposition Numbers in CCDC	2,215,024	2,215,025

In both complexes **2** and **3**, two cyclic diphosphine ligands coordinate two gold(I) ions via the P,P-bridging mode, forming a 12-membered metallocacyclic ring. In the cation of **2**, the linear geometry of both gold(I) ions is realized by two phosphorus atoms of two diphosphine ligands. Two chloride counterions are located in the outer sphere. Two gold ions in the neutral complex **3** have a trigonal geometry formed by two phosphorus atoms of two diphosphine ligands and the iodo-ligand (Au-I bond is 3.168(1) Å, Table S1). The linear or T-shaped ligand environment, is often observed for the gold(I) atoms in complexes with various ligands [21,34]. Unlike the previously reported dimeric gold(I) complexes of *N*-aryl substituted 1,5-diaza-3,7-diphosphacyclooctanes, the geometry of the ligand environment of the gold(I) ions in complexes **2** and **3** is slightly distorted from the ideal linear or T-shaped geometry, due to the aurophilic interactions. The distances between the two gold(I) ions in complexes **2** and **3** (2.9977(6) and 3.1680(5) Å respectively) are less than the sum of the van der Waals radii [35,36] and drastically differ from the Au ··· Au distances observed in the previously reported dimeric gold(I) complexes of *N*-aryl substituted 1,5-diaza-3,7-diphosphacyclooctanes: 3.4994(5) Å (for the gold(I) chloride complex) and 4.8921(5) Å (for the gold(I) iodide complex) (Figure 2) [28].

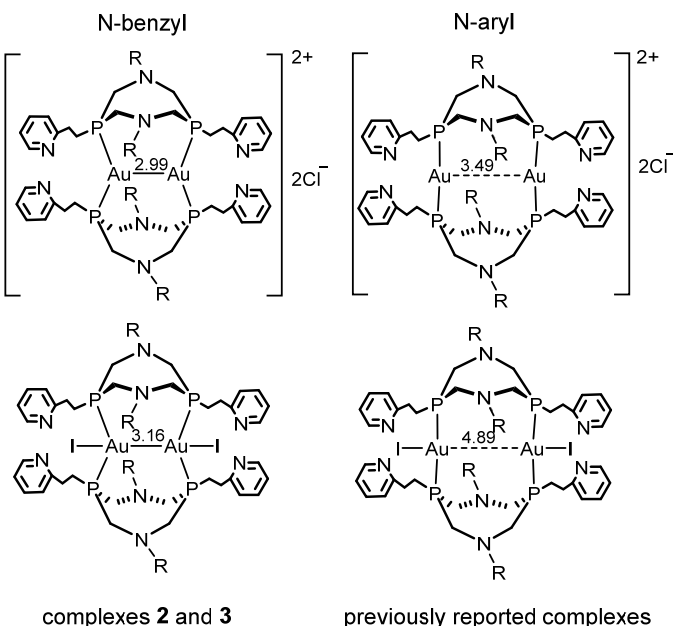


**Figure 2.** Schematic illustration of the structures of dimeric gold(I) complexes with *N*-alkyl and *N*-aryl substituted 1,5-diaza-3,7-diphosphacyclooctanes.

The initial uncoordinated *N,N*-dibenzhydryl-P,P-bis(pyridylethyl) diazadiphosphacyclooctane exists in the “crown” conformation with a mutual orientation of two phosphorus lone pairs leaning towards each other [30], that are pre-organized for the close arrangement of the two coordinated gold(I) ions and the realization of the aurophilic interaction. Oppo-

sitely, the phosphorus lone pairs of *N*-aryl substituted 1,5-diaza-3,7-diphosphacyclooctanes are oriented in a nearly parallel manner, and therefore the aurophilic interactions were not observed in the molecular structures for the previously reported dimeric gold(I) complexes. [28,31]

Two 8-membered cyclic ligands in the complexes **2** and **3** have a twisted “chair-boat” conformation with an equatorial orientation of the pyridylethyl substituents at the phosphorus atoms and the benzhydryl substituent at the nitrogen atom in a “chair” part of the ligands and an axial position of the benzhydryl substituent in a “boat” part of the ligands. In the complex **2**, the “chair” parts of the two ligands are located on the one side of the metallocycle plane, whereas the “boat” parts of the two ligands are located on the other side of the metallocycle plane (“*cis*-position”). One of the gold atoms is in a short contact with a chloride ion ( $\text{Au} \cdots \text{Cl}$  distance 3.03 Å), while no chloride ion is observed at the second gold(I) ion. The equatorial *sin*-orientation of the two sterically hindered *N*-benzhydryl substituents in the complex **2** probably prevents the close arrangement of the chloride anions to the gold(I) atom from the “chair” side of the molecule, whereas the axial *anti*-orientation of *N*-benzhydryl substituents on the “boat” side allows to locate the chloride or solvent molecules nearly to the gold(I) cation. In the gold(I) iodide complex **3**, the “chair” part of one of the ligands and the “boat” part of the other ligand are located on each side of the metallocycle plane (“*trans*-position”). In this case, there are no steric restrictions in the coordination of the iodo-ligands to the gold atom.

*Photophysical study.* The UV/Vis spectrum of complexes **2** and **3** measured at the DCM display absorption bands at ca. 250 and 330 (2) or 385 (3) nm, are also appropriately predicted, computationally (Figure 3).

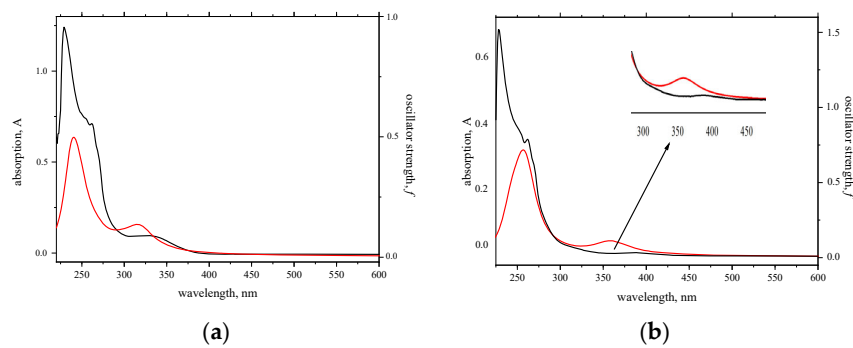


**Figure 3.** Experimental (black) and calculated (red) UV/Vis spectra of complex **2** (a) and **3** (b).

The UV/Vis spectrum, simulated for the optimized structure of complex **2** with one chloride ion coordinated to Au(I) (which was applied for the optimization, according to the XRD structure) and the second chloride ion localized in the outer sphere, matches well with the experimental curve (Figure 3a). According to the computations, the longest wavelength absorption band (ca. 330 nm) is caused by the transitions from HOMO-3 to LUMO and from HOMO-2 to LUMO. Analysis of these frontier orbitals (Figure 4) suggests the mixed ( $M+X$ )LCT and intraligand charge transfer origins of the band.

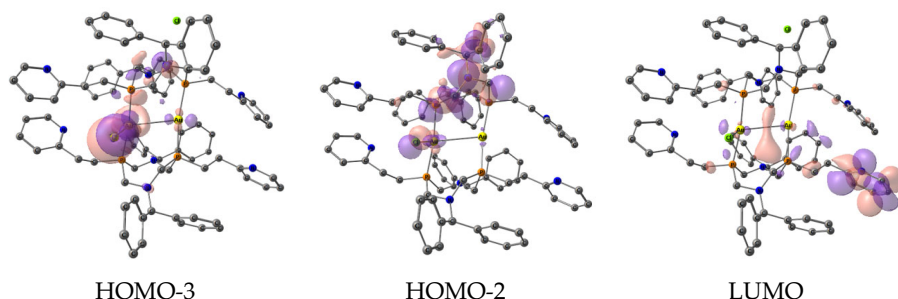


**Figure 4.** Frontier orbitals of the singlet ground states ( $S_0$ ) at the optimized  $S_0$  of complex **2**.

The longest wavelength absorption band of complex **3** at 385 nm, corresponds to the  $S_0$ - $S_1$  transition at 360 nm, contributed mostly by the charge transfer from the highest occupied to the lowest unoccupied orbitals (HOMO to LUMO, Figure 5). It should be mentioned that for the previously reported *N*-aryl substituted gold(I) complexes [28], the corresponding absorption bands appeared as tails at 350–370 nm. The more pronounced absorption for complex **3** is most probably related with the aurophilic interactions in the case of complex **3**: Au…Au distance in the ground state is predicted to be equal to 3.19 Å for **3**, compared to 3.80 for the previously reported complex [28].

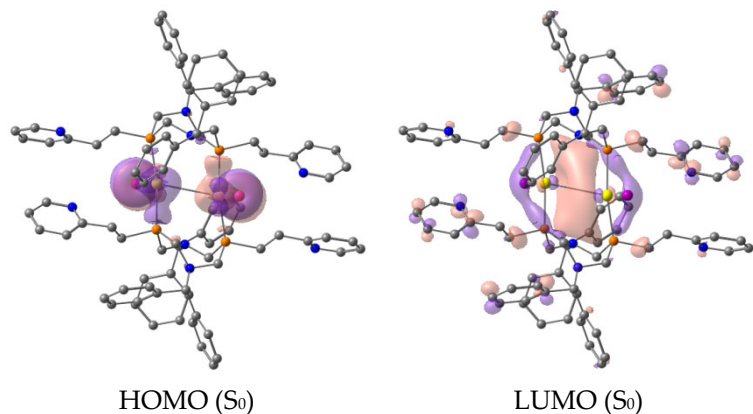


**Figure 5.** Frontier orbitals of the singlet ground states ( $S_0$ ) at the optimized  $S_0$  of complex **3**.

The dried powders of complexes **2** and **3** display a moderate emission in the solid state in the bluish-green region of the spectra at room temperature (Figure 6). The emission maxima of chloride complex **2** at ca. 505 nm is blue shifted, in comparison with the iodide complex **3** ( $\lambda_{\text{em}}$  535 nm). The excitation spectra of both complexes are similar and represent the broad bands of excitation with the maxima in the range of 350–410 nm. The UV/vis absorption spectra of complexes **2** and **3** measured in the solid-state (Figures S3 and S4) are similar to the excitation spectra. The emission lifetimes with the values of ca. 0.35 (**2**) and 2.14 (**3**) microseconds (Figures S5 and S6) indicate the phosphorescent origin of the luminescence of the complexes. Notably, that the gold(I) complexes often demonstrate a phosphorescence with the fast luminescence decay values of hundreds of nanoseconds [6,37,38].

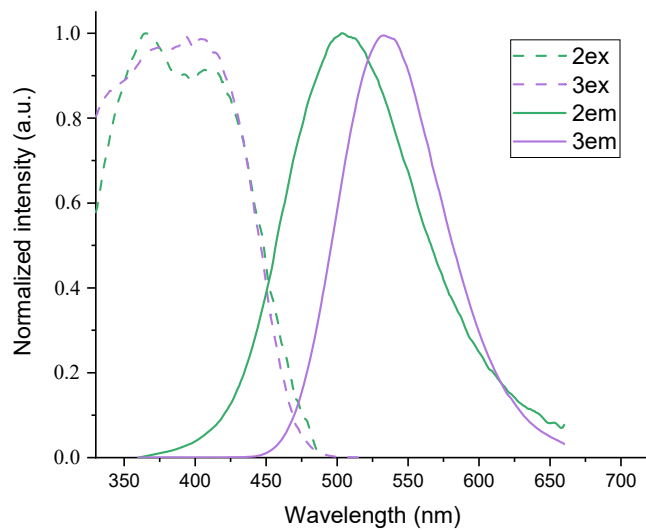


**Figure 6.** Solid state excitation and emission spectra of complexes **2** and **3** at room temperature.

The origins of the observed emission were estimated quantum chemically on the example of complex **3** with iodide ions. The analysis of the frontier orbitals suggests

the dominating  ${}^3(M+X)C$  (metal-halide-centered) nature of the transition with a minor contribution of  ${}^3MLCT$  (metal-to-ligand charge transfer). The computations predict the  $T_1-S_0$  transition at 512 nm for **3** which is in agreement with the experimental emission (535 nm). The  $Au \cdots Au$  distance in the triplet state of **3** is significantly shortened, compared to the ground singlet state ( $3.19 \text{ \AA} \rightarrow 2.87 \text{ \AA}$ ). The shortening of the  $Au \cdots Au$  distances leads to the strengthening of the aurophilic interactions and the localization of both the highest occupied and lowest unoccupied orbitals (HOMOs and LUMOs) at the  $Au_2I_2$  cluster of complex **3** (Figure 7).

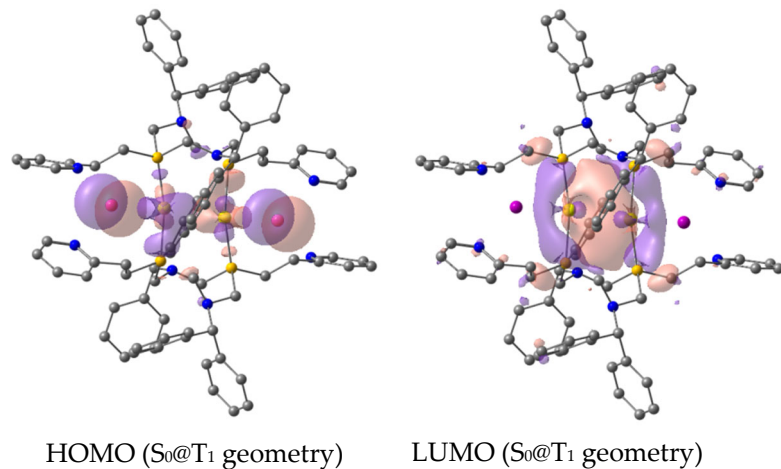


**Figure 7.** Frontier orbitals of the singlet ground states ( $S_0$ ) at the optimized  $T_1$  ( $S_0@T_1$ , bottom) geometries of complex **3**.

The TDDFT computations predict the strong difference in the  $Au \cdots Au$  distances in the ground states of the previously reported *N*-aryl substituted gold iodide complexes, compared to complex **3** ( $3.19 \text{ \AA}$  for **3** vs.  $3.8 \text{ \AA}$  for the previous reported complexes), whereas the  $Au \cdots Au$  distances in the excited states have a comparable value (ca.  $2.9 \text{ \AA}$ ). The decrease of the geometry changes upon the excitation of the molecule leads to the decrease of the Stokes shift (150 nm) (Figure 8), which is observed, experimentally.

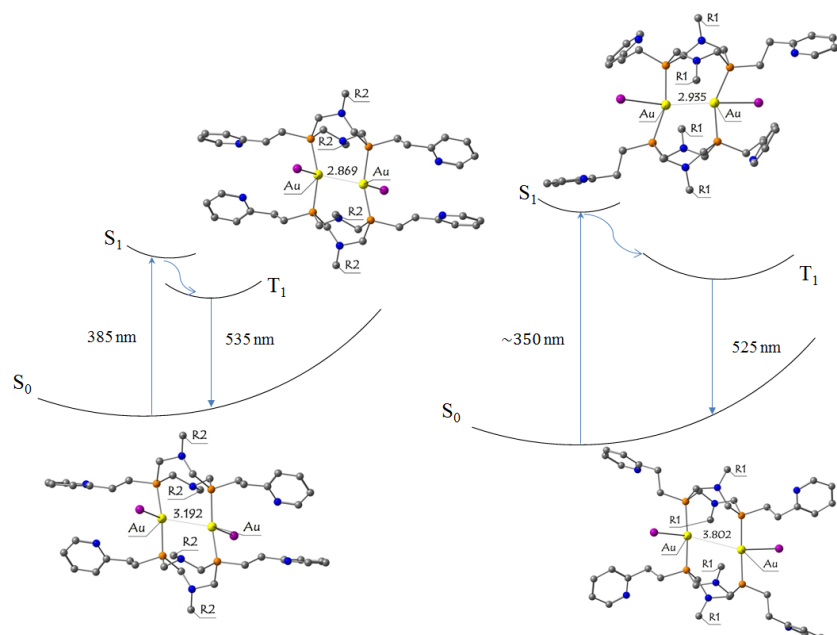


**Figure 8.** Principal potential curves of the emission transitions of the molecules with a low geometry difference (**left**) and a large geometry difference (**right**) upon excitation.

For the optimized structures received from the XRD data, the computations predict the  $T_1-S_0$  transition at 649 nm, which does not meet the experimental observations. Therefore, the quantum-chemically triplet states have been considered for other two possible structures: for dication of complex **2** without counterions (**2a**, Figure S7) and for the structure, obtained by the computational replacement of the iodide anions in the optimized structure of **3**, by chloride ions (**2b**, Figure S7). The computations predict the  $T_1-S_0$  transition at 462 nm for **2a** and 513 nm for **2b**. The experimentally observed emission at 505 nm is close to the structure **2b**, however the existence of the triplet state of **2a** cannot be excluded. The analysis of the frontier orbitals shows that model emission originates from  $^3L(X+M)CT$  for **2a** transitions and from  $^3(M+X)C$  transitions for **2b** (Figure S8). We attempted to interpret the photophysical properties of **2** by the comparison of **2** with the previously reported Au(I) chloride dimeric complex of *N*-*p*-tolyl substituted 1,5-diaza-3,7-diphosphacyclooctane [28] and with complex **3**. Taking into account that the photophysical experiments and the TDDFT calculations predict the  $^3(M+X)C$  origin of the emission of complex **3** and the previously reported complexes [28], the emission of **2** could also be suggested to be caused by the  $^3(M+X)C$  transitions. The previously reported *N*-aryl substituted dimeric Au(I) chloride complexes displayed a green emission with the maxima at 540–548 nm [28]. The difference between the Au  $\cdots$  Au distances in the ground state and the excited state ( $3.49\text{ \AA} \rightarrow 2.84\text{ \AA}$ ) of the previously reported chloride complex [28] is stronger, than that for complex **2**, due to the shorter Au  $\cdots$  Au distance in the ground state of **2** ( $3.17\text{ \AA}$ ). Possibly, the short Au  $\cdots$  Au distance of complex **2** is the main reason for the strong hypsochromic shift of the emission band up to 505 nm relative to the previously reported gold(I) dimeric complex of *N,N*-*p*-tolyl substituted 1,5-diaza-3,7-diphosphacyclooctanes.

### 3. Materials and Methods

All reactions and purifications were carried out under a dry argon atmosphere using standard vacuum-line techniques. The commercially available solvents were purified, dried, deoxygenated, and distilled before use. Au(tht)Cl was obtained according to the previously reported procedure [39]. 1,5-Bis(benzhydryl)-3,7-bis(2-(pyridine-2'-yl)ethyl)-1,5-diaza-3,7-diphosphacyclooctane was synthesized and purified, according to the experimental procedures described, previously [28]. All other compounds are commercially available.

$^1H$  NMR (600.1 MHz) and  $^{31}P$  NMR (242.9 MHz) spectra were recorded on a Bruker Avance 600 spectrometer and  $^1H$  NMR (400.13 MHz) and  $^{31}P$  NMR (161.96 MHz) spectra were recorded on a Bruker Avance 400 spectrometer using the residual solvent as an internal reference for  $^1H$  ( $\delta = 1.94$  ppm in  $CD_3CN$ ,  $\delta = 7.26$  in  $CDCl_3$ ) and 85% aqueous solution of  $H_3PO_4$  as an external reference for  $^{31}P$ . The chemical shifts are reported in ppm and the coupling constants ( $J$ ) are reported in Hz. The ESI MS measurements were performed using an AmaZon X ion trap mass spectrometer in the positive and negative modes. The mass spectra are given as  $m/z$  values and relative intensities ( $I_{rel}$ , %). Acetonitrile was used as a solvent for the mass spectrometry measurements. The CHN-elemental analysis was carried out on the EuroEA3028-HT-OM «Eurovector SpA». The elemental analysis for halogen was carried out by the determination of the quantitative content of the halogens, according to the Schöniger method. The elemental analysis for the metal traces and phosphorus was carried out using the gravimetric method of analysis.

**Photophysical measurements.** The electronic absorption (UV-Vis) spectra were recorded at room temperature on a PerkinElmer Lambda 35 spectrometer with a scan speed of 480 nm/min, using a spectral width of 1 nm. All samples were prepared as solutions in dichloromethane with concentrations of  $\sim 10^{-5}\text{ mol}\cdot L^{-1}$  and placed in 10 mm quartz cells. The solid-state excitation and emission spectra were measured on Fluorolog-3 (Horiba) and Fluorolog QM-75-22-C (Horiba) spectrofluorimeters. LED (370 nm, pulse duration 1.2 ns) was used to carry out lifetime measurements at room temperature. The quantum yields of luminescence were measured using the integration sphere QuantaPhi (Horiba).

**Computational Methods.** Quantum chemical calculations were performed with the Gaussian [40] suite of programs. The ground/excited-state structures were optimized

with the use of the hybrid PBE0 functional [41] and Ahlrichs' triple- $\zeta$  def-TZVP AO basis set [42]. In all of the geometry optimizations, the D3 approach [43] to describe the London dispersion interactions, together with the Becke–Johnson damping function [44–46] were employed as implemented in the Gaussian 16 program. The time-dependent density functional response theory (TDDFT) has been employed to compute the vertical excitation energies (i.e., absorption wavelengths) and the oscillator strengths for the ground-state optimized geometries in the gas phase, the 50 lowest singlet excited states were taken into account. The procedure was analogous to the one described elsewhere [47]. The calculated spectra were shifted by −0.24 eV. The vertical T<sub>1</sub>–S<sub>0</sub> transition energies were also computed within the TDDFT approach at the PBE0/def-TZVP level at the triplet geometries optimized by UPBE0–D3(BJ)/def-TZVP level of theory.

**Single Crystal X-ray Diffraction.** The X-ray diffraction study of complex **2** was conducted on a Bruker D8 QUEST automated three-circle diffractometer with a PHOTON III area detector and an I $\mu$ S DIAMOND microfocus X-ray source ([MoK $\alpha$ ] = 0.71073 Å) at 110(2) K. The single crystal **3** was studied on a Rigaku XtaLAB Synergy S with a c HyPix area detector and an PhotonJet microfocus X-ray source (CuK $\alpha$ ) = 1.54184 Å) at 100(2) K. The diffraction data were collected and processed using APEX3 and CrysAlisPro packages. The structures were solved by direct methods with the SHELXT program [48] and were refined by the least-squares method on F<sup>2</sup> using the SHELXL software [49]. The non-hydrogen atoms were refined in the anisotropic approximation. All hydrogen atoms were calculated geometrically and refined using the riding model. In crystal **2**, was found the total potential solvent accessible void volume (SOLV-Map Value) 454 Å<sup>3</sup>, but the solvate molecules were not found from the different Fourier maps of electron density, and the final stages of the structure refinement were performed using the SQUEEZE procedure of the PLATON program [50]. Crystal **2** is a solvate with CH<sub>2</sub>Cl<sub>2</sub> and an unspecified solvent. The crystal data of structures **1** and **3** were deposited with the Cambridge Crystallographic Data Centre; the CCDC codes and the most important characteristics are listed in Table 1.

#### Synthetic Procedures.

**Complex 2.** A solution of [AuCl(tht)] (0.046 g, 0.145 mmol) in acetone (5 mL) was added to a solution of **1** (0.100 g, 0.145 mmol) in acetone (5 mL). The reaction mixture was stirred at room temperature for 2 h, the resulting white precipitate was isolated by filtration, washed with acetone, and dried under a reduced pressure. The yield was 0.100 g (76%). The elemental analysis, calculated for C<sub>88</sub>H<sub>92</sub>N<sub>8</sub>P<sub>4</sub>Au<sub>2</sub>Cl<sub>2</sub> [1850]: C 57.12, H 5.01, N 6.06, P 6.70, Au 21.29, Cl 3.83%. Found: C 57.27, H 5.07, N 6.13, P 6.56, Au 21.25, Cl 3.71%. MS (ESI<sub>pos</sub>, m/z (I<sub>rel</sub>, %), ion): 889 (100) [M-2Cl]<sup>2+</sup>. <sup>1</sup>H NMR (CD<sub>2</sub>Cl<sub>2</sub>, ppm):  $\delta$ <sub>H</sub> 8.31 (d, <sup>3</sup>J<sub>HH</sub> = 4.44 Hz, 2H, H-Py), 7.47–7.58 (m, 8H, H-Bnz), 7.43 (ddd, <sup>3</sup>J<sub>HH</sub> = 7.52 Hz, <sup>3</sup>J<sub>HH</sub> = 7.52 Hz, <sup>4</sup>J<sub>HH</sub> = 1.71 Hz, 2H, H-Py), 7.24–7.32 (m, 8H, H-Bnz), 7.15–7.22 (m, 4H, H-Bnz), 6.99–7.06 (m, 2H, H-Py), 6.86 (d, 2H, <sup>3</sup>J<sub>HH</sub> = 7.86 Hz, H-Py), 5.33–5.39 (m, 2H, H-Bnz), 3.85–4.15 (m, 4H, H-PCH<sub>2</sub>N), 3.72–3.84 (m, 4H, H-PCH<sub>2</sub>N), 2.55–2.71 (m, 4H, H-CH<sub>2</sub>CH<sub>2</sub>P), 1.93–2.05 (m, 4H, H-CH<sub>2</sub>CH<sub>2</sub>P)). <sup>31</sup>P{<sup>1</sup>H} NMR (CD<sub>2</sub>Cl<sub>2</sub>, ppm.):  $\delta$ <sub>P</sub> 31.04 ppm.

**Complex 3.** A solution of AuI (0.047 g, 0.145 mmol) in acetone (5 mL) was added to a solution of **1** (0.100 g, 0.145 mmol) in acetone (5 mL). The reaction mixture was stirred at room temperature for 2 h, the resulting white precipitate was isolated by filtration, washed with acetone, and dried under a reduced pressure. The yield was 0.150 g (90%). Elemental analysis, calculated for C<sub>88</sub>H<sub>92</sub>N<sub>8</sub>P<sub>4</sub>Au<sub>2</sub>I<sub>2</sub> [2033]: C 51.98, H 4.56, N 5.51, P 6.09, Au 19.37, I 12.48%. Found C 52.04, H 4.59, N 5.48, P 6.02, Au 19.41, I 12.45%. MS (ESI<sub>pos</sub>, m/z (I<sub>rel</sub>, %), ion): 1905 (100) [M-I]<sup>+</sup>, 889 (50) [M-2I]<sup>2+</sup>. <sup>1</sup>H NMR (CD<sub>2</sub>Cl<sub>2</sub>, ppm):  $\delta$ <sub>H</sub> 8.26–8.32 (m, 2H, H-Py), 7.41–7.52 (m, 8H, H-Bnz), 7.35–7.40 (m, 2H, H-Py), 7.27–7.34 (m, 8H, H-Bnz), 7.16–7.27 (m, 4H, H-Bnz), 6.95–7.01 (m, 2H-Py), 6.80 (d, <sup>3</sup>J<sub>HH</sub> = 8.07 Hz, 2H, H-Py), 3.92–4.24 (m, 4H, H-PCH<sub>2</sub>N), 3.52–3.64 (m, 4H, H-PCH<sub>2</sub>N), 2.58–2.70 (m, 4H, H-CH<sub>2</sub>CH<sub>2</sub>P), 1.91–2.07 (m, 4H, H-CH<sub>2</sub>CH<sub>2</sub>P)). <sup>31</sup>P{<sup>1</sup>H} NMR (CD<sub>2</sub>Cl<sub>2</sub>, ppm.):  $\delta$ <sub>P</sub> 32.05.

#### 4. Conclusions

In summary, new dimeric gold(I) chloride and gold(I) iodide complexes with *N,N*-bis(benzhydryl) substituted 1,5-diaza-3,7-diphosphacyclooctanes were obtained. The XRD structures of the complexes demonstrate the strong aurophilic interactions, which are strengthened by the preorganized initial geometry of the ligand. The thorough analysis of the structures and the luminescence of the gold complexes, based on *N,N*-diaryl and *N,N*-dibenzhydryl substituted 1,5,3,7-diazadiphosphacyclooctanes reveals the strong influence of the mutual orientation of the phosphorus lone pairs in the initial ligands on the geometry of their dimeric gold complexes. They are directed to each other through the arrangement of the phosphorus lone pairs in *N,N*-dibenzhydryl substituted 1,5,3,7-diazadiphosphacyclooctanes, and is preorganized for the realization of the strong aurophilic interactions in the complexes. It plays a significant role for the emission properties, mostly by the increase of the rigidity of the molecule, which results in the slight geometrical changes during the transition from the ground to the excited states of the complexes. It reflects the decreased Stokes shift in the gold iodide complex and in the hypsochromic shift of the emission of the gold chloride complex.

**Supplementary Materials:** The following supporting information can be downloaded at: <https://www.mdpi.com/article/10.3390/inorganics10120224/s1>.

**Author Contributions:** Conceptualization, I.D.S., T.P.G., E.I.M. and A.A.K.; methodology, A.I.F., I.R.D., I.A.L., D.R.I. and I.E.K.; formal analysis, I.E.K., I.A.L. and D.R.I.; investigation, I.D.S., T.P.G., A.I.F. and I.R.D.; writing—original draft preparation, I.D.S., T.P.G. and E.I.M.; writing—review and editing, E.I.M. and A.A.K.; project administration, A.A.K. All authors have read and agreed to the published version of the manuscript.

**Funding:** The work was financially supported by the Russian Science Foundation (grant 22-13-00147). The physical experiments were carried out at the Assigned Spectral-Analytical Center of FRC Kazan Scientific Center of RAS. The photoluminescence studies were performed at the Centre for Optical and Laser Materials Research of Saint Petersburg State University with financial support from St. Petersburg State University (project No 93021679).

**Data Availability Statement:** Cambridge Crystallographic Data Centre #2215024; #2215025.

**Conflicts of Interest:** The authors declare no conflict of interest.

#### References

- Mirzadeh, N.; Privér, S.H.; Blake, A.J.; Schmidbaur, H.; Bhargava, S.K. Innovative Molecular Design Strategies in Materials Science Following the Auophilicity Concept. *Chem. Rev.* **2020**, *120*, 7551–7591. [[CrossRef](#)] [[PubMed](#)]
- He, X.; Yam, V.W.W. Luminescent Gold(I) Complexes for Chemosensing. *Coord. Chem. Rev.* **2011**, *255*, 2111–2123. [[CrossRef](#)]
- Tiekink, E.R.T.; Kang, J.G. Luminescence Properties of Phosphinegold(I) Halides and Thiolates. *Coord. Chem. Rev.* **2009**, *253*, 1627–1648. [[CrossRef](#)]
- Pyykkö, P. Theoretical Chemistry of Gold. III. *Chem. Soc. Rev.* **2008**, *37*, 1967–1997. [[CrossRef](#)] [[PubMed](#)]
- Van Zyl, W.E.; López-De-Luzuriaga, J.M.; Fackler, J.P. Luminescence Studies of Dinuclear Gold(I) Phosphor-1,1-Dithiolate Complexes. *J. Mol. Struct.* **2000**, *516*, 99–106. [[CrossRef](#)]
- Penney, A.A.; Sizov, V.V.; Grachova, E.V.; Krupenya, D.V.; Gurzhiy, V.V.; Starova, G.L.; Tunik, S.P. Auophilicity in Action: Fine-Tuning the Gold(I)-Gold(I) Distance in the Excited State to Modulate the Emission in a Series of Dinuclear Homoleptic Gold(I)-NHC Complexes. *Inorg. Chem.* **2016**, *55*, 4720–4732. [[CrossRef](#)]
- Yang, D.; Liu, H.; Wang, D.L.; Lu, Y.; Zhao, X.L.; Liu, Y. Au-Complex Containing Phosphino and Imidazolyl Moieties as a Bi-Functional Catalyst for One-Pot Synthesis of Pyridine Derivatives. *J. Mol. Catal. A Chem.* **2016**, *424*, 323–330. [[CrossRef](#)]
- Forfar, L.C.; Zeng, D.; Green, M.; McGrady, J.E.; Russell, C.A. Probing the Structure, Dynamics, and Bonding of Coinage Metal Complexes of White Phosphorus. *Chem. A Eur. J.* **2016**, *22*, 5397–5403. [[CrossRef](#)]
- Zhang, J.; Zou, H.; Lei, J.; He, B.; He, X.; Sung, H.H.Y.; Kwok, R.T.K.; Lam, J.W.Y.; Zheng, L.; Tang, B.Z. Multifunctional AuI-Based AIEgens: Manipulating Molecular Structures and Boosting Specific Cancer Cell Imaging and Theranostics. *Angew. Chem. Int. Ed.* **2020**, *59*, 7097–7105. [[CrossRef](#)]
- Moreno-Alcantar, G.; Romo-Islas, G.; Flores-Alamo, M.; Torrens, H. Auophilicity vs. Thiophilicity: Directing the Crystalline Supramolecular Arrangement in Luminescent Gold Compounds. *New J. Chem.* **2018**, *42*, 7845–7852. [[CrossRef](#)]
- Czerwieniec, R.; Hofbeck, T.; Crespo, O.; Laguna, A.; Concepción Gimeno, M.; Yersin, H. The Lowest Excited State of Brightly Emitting Gold(I) Triphosphine Complexes. *Inorg. Chem.* **2010**, *49*, 3764–3767. [[CrossRef](#)]

12. Fackler, J.P.; Grant, T.A.; Hanson, B.E.; Staples, R. Characterization of the Luminescent, Homoleptic, Three-Coordinate, Water Soluble Au(I) Complex of Trisulfonated Triphenylphosphine (TPPTS) as the Cesium Salt, CS<sub>8</sub>[Au(TPPTS)<sub>3</sub>]·5.25 H<sub>2</sub>O. *Gold Bull.* **1999**, *32*, 20–23. [[CrossRef](#)]
13. Wenger, O.S. Vapochromism in Organometallic and Coordination Complexes: Chemical Sensors for Volatile Organic Compounds. *Chem. Rev.* **2013**, *113*, 3686–3733. [[CrossRef](#)]
14. Elistratova, J.; Faizullin, B.; Shamsutdinova, N.; Gubaiddullin, A.; Strelnik, I.; Babaev, V.; Kholin, K.; Nizameev, I.; Musina, E.; Khairullin, R.; et al. Synthesis of Au(I) Complex-Based Aqueous Colloids for Sensing of Biothiols. *Inorg. Chim. Acta* **2019**, *485*, 26–32. [[CrossRef](#)]
15. Strelnik, I.D.; Sizov, V.V.; Gurzhiy, V.V.; Melnikov, A.S.; Kolesnikov, I.E.; Musina, E.I.; Karasik, A.A.; Grachova, E.V. Binuclear Gold(I) Phosphine Alkynyl Complexes Templatized on a Flexible Cyclic Phosphine Ligand: Synthesis and Some Features of Solid-State Luminescence. *Inorg. Chem.* **2020**, *59*, 244–253. [[CrossRef](#)]
16. Strelnik, I.D.; Gurzhiy, V.V.; Sizov, V.V.; Musina, E.I.; Karasik, A.A.; Tunik, S.P.; Grachova, E.V. A Stimuli-Responsive Au(I) Complex Based on an Aminomethylphosphine Template: Synthesis, Crystalline Phases and Luminescence Properties. *CrystEngComm* **2016**, *18*, 7629–7635. [[CrossRef](#)]
17. Grachova, E.V. Design of Supramolecular Cluster Compounds of Copper Subgroup Metals Based on Polydentate Phosphine Ligands. *Russ. J. Gen. Chem.* **2019**, *89*, 1102–1114. [[CrossRef](#)]
18. Barnard, P.J.; Wedlock, L.E.; Baker, M.V.; Berners-Price, S.J.; Joyce, D.A.; Skelton, B.W.; Steer, J.H. Luminescence Studies of the Intracellular Distribution of a Dinuclear Gold(I) N-Heterocyclic Carbene Complex. *Angew. Chem. Int. Ed.* **2006**, *45*, 5966–5970. [[CrossRef](#)]
19. Revol, G.; McCallum, T.; Morin, M.; Gagosc, F.; Barriault, L. Photoredox Transformations with Dimeric Gold Complexes. *Angew. Chem. Int. Ed.* **2013**, *52*, 13342–13345. [[CrossRef](#)]
20. Si, X.; Zhang, L.; Wu, Z.; Rudolph, M.; Asiri, A.M.; Hashmi, A.S.K. Visible Light-Induced  $\alpha$ -C(Sp<sub>3</sub>)-H Acetalization of Saturated Heterocycles Catalyzed by a Dimeric Gold Complex. *Org. Lett.* **2020**, *22*, 5844–5849. [[CrossRef](#)]
21. Pal, S.; Kathewad, N.; Pant, R.; Khan, S. Synthesis, Characterization, and Luminescence Studies of Gold(I) Complexes with PNP- and PNB-Based Ligand Systems. *Inorg. Chem.* **2015**, *54*, 10172–10183. [[CrossRef](#)] [[PubMed](#)]
22. Jobbág, C.; Baranyai, P.; Marsi, G.; Rácz, B.; Li, L.; Naumov, P.; Deák, A. Novel Gold(i) Diphosphine-Based Dimers with Auophilicity Triggered Multistimuli Light-Emitting Properties. *J. Mater. Chem. C Mater.* **2016**, *4*, 10253–10264. [[CrossRef](#)]
23. Pan, Q.J.; Zhang, H.X. Auophilic Attraction and Excited-State Properties of Binuclear Au(I) Complexes with Bridging Phosphine and/or Thiolate Ligands: An Ab Initio Study. *J. Chem. Phys.* **2003**, *119*, 4346–4352. [[CrossRef](#)]
24. Moreno-Alcántar, G.; Salazar, L.; Romo-Islas, G.; Flores-Álamo, M.; Torrens, H. Exploring the Self-Assembled Tacticity in Auophilic Polymeric Arrangements of Diphosphanegold(I) Fluorothiolates. *Molecules* **2019**, *24*, 4422. [[CrossRef](#)] [[PubMed](#)]
25. Leung, K.H.; Phillips, D.L.; Tse, M.C.; Che, C.M.; Miskowski, V.M. Resonance Raman Investigation of the Au(I)—Au(I) Interaction of the 1[Dσ\*ρσ] Excited State of Au<sub>2</sub>(Dcpm)<sub>2</sub>(ClO<sub>4</sub>)<sub>2</sub> (Dcpm = Bis(Dicyclohexylphosphine)Methane). *J. Am. Chem. Soc.* **1999**, *121*, 4799–4803. [[CrossRef](#)]
26. Elistratova, J.; Strelnik, I.; Brylev, K.; Shestopalov, M.A.; Gerasimova, T.; Babaev, V.; Kholin, K.; Dobrynnin, A.; Musina, E.; Katsyuba, S.; et al. Novel Water Soluble Cationic Au(I) Complexes with Cyclic PNPN Ligand as Building Blocks for Heterometallic Supramolecular Assemblies with Anionic Hexarhenium Cluster Units. *J. Lumin.* **2018**, *196*, 485–491. [[CrossRef](#)]
27. Elistratova, J.; Faizullin, B.; Strelnik, I.; Gerasimova, T.; Khairullin, R.; Sapunova, A.; Voloshina, A.; Mukhametzyanov, T.; Musina, E.; Karasik, A.; et al. Impact of Oppositely Charged Shell and Cores on Interaction of Core-Shell Colloids with Differently Charged Proteins as a Route for Tuning of the Colloids Cytotoxicity. *Colloids Surf. B Biointerfaces* **2020**, *196*, 111306. [[CrossRef](#)]
28. Dayanova, I.R.; Shamsieva, A.V.; Strelnik, I.D.; Gerasimova, T.P.; Kolesnikov, I.E.; Fayzullin, R.R.; Islamov, D.R.; Saifina, A.F.; Musina, E.I.; Hey-Hawkins, E.; et al. Assembly of Heterometallic AuICu<sub>2</sub>I<sub>2</sub>Cores on the Scaffold of NPPN-Bridging Cyclic Bisphosphine. *Inorg. Chem.* **2021**, *60*, 5402–5411. [[CrossRef](#)]
29. Strelnik, I.D.; Dayanova, I.R.; Krivolapov, D.B.; Litvinov, I.A.; Musina, E.I.; Karasik, A.A.; Sinyashin, O.G. Unpredicted Concurrency between P,P-Chelate and P,P-Bridge Coordination Modes of 1,5-DiR-3,7-Di(Pyridine-2-Yl)-1,5-Diaza-3,7-Diphosphacyclooctane Ligands in Copper(I) Complexes. *Polyhedron* **2018**, *139*, 1–6. [[CrossRef](#)]
30. Strelnik, I.D.; Musina, E.I.; Ignatieva, S.N.; Balueva, A.S.; Gerasimova, T.P.; Katsyuba, S.A.; Krivolapov, D.B.; Dobrynnin, A.B.; Bannwarth, C.; Grimme, S.; et al. Pyridyl Containing 1,5-Diaza-3,7-Diphosphacyclooctanes as Bridging Ligands for Dinuclear Copper(I) Complexes. *Z. Anorg. Allg. Chem.* **2017**, *643*, 895–902. [[CrossRef](#)]
31. Strelnik, I.D.; Dayanova, I.R.; Kolesnikov, I.E.; Fayzullin, R.R.; Litvinov, I.A.; Samigullina, A.I.; Gerasimova, T.P.; Katsyuba, S.A.; Musina, E.I.; Karasik, A.A. The Assembly of Unique Hexanuclear Copper(I) Complexes with Effective White Luminescence. *Inorg. Chem.* **2019**, *58*, 1048–1057. [[CrossRef](#)]
32. Musina, E.I.; Khrizanforova, V.V.; Strelnik, I.D.; Valitov, M.I.; Spiridonova, Y.S.; Krivolapov, D.B.; Litvinov, I.A.; Kadirov, M.K.; Loennecke, P.; Hey-Hawkins, E.; et al. New Functional Cyclic Aminomethylphosphine Ligands for the Construction of Catalysts for Electrochemical Hydrogen Transformations. *Chem. A Eur. J.* **2014**, *20*, 3169–3182. [[CrossRef](#)]
33. Karasik, A.A.; Musina, E.I.; Balueva, A.S.; Strelnik, I.D.; Sinyashin, O.G. Cyclic Aminomethylphosphines as Ligands. Rational Design and Unpredicted Findings. *Pure Appl. Chem.* **2017**, *89*, 293–309. [[CrossRef](#)]

34. Lim, S.H.; Schmitt, J.C.; Shearer, J.; Jia, J.H.; Olmstead, M.M.; Fettinger, J.C.; Balch, A.L. Crystallographic and Computational Studies of Luminescent, Binuclear Gold(I) Complexes,  $\text{Au}_2(\text{I})(\text{Ph}_2\text{P}(\text{CH}_2)(n)\text{PPh}_2)_2\text{I}_2$  ( $n = 3–6$ ). *Inorg. Chem.* **2013**, *52*, 823–831. [[CrossRef](#)]
35. Alvarez, S. A Cartography of the van Der Waals Territories. *Dalton. Trans.* **2013**, *42*, 8617–8636. [[CrossRef](#)]
36. Bondi, A. Van Der Waals Volumes and Radii. *J. Phys. Chem.* **1964**, *68*, 441–451. [[CrossRef](#)]
37. Ma, Y.; Zhou, X.; Shen, J. Triplet luminescent dinuclear-gold(I) complex-based light-emitting diodes with low turn-on voltage. *Appl. Phys. Lett.* **1999**, *74*, 1361. [[CrossRef](#)]
38. Schneider, J.; Lee, Y.A.; Pérez, J.; Brennessel, W.W.; Flaschenriem, C.; Eisenberg, R. Strong Intra- and Intermolecular Auophilic Interactions in a New Series of Brilliantly Luminescent Dinuclear Cationic and Neutral Au(I) Benzimidazolethiolate Complexes. *Inorg. Chem.* **2008**, *47*, 957–968. [[CrossRef](#)]
39. Uson, R.; Laguna, A.; Laguna, M.; Briggs, D.A.; Murray, H.H.; Fackler, J.P. (Tetrahydrothiophene)Gold(I) or Gold(III) Complexes. *Inorg. Synth.* **1989**, *26*, 85–91. [[CrossRef](#)]
40. Gaussian 16, Revision C.01, Frisch, M.J.; Trucks, G.W.; Schlegel, H.B.; Scuseria, G.E.; Robb, M.A.; Cheeseman, J.R.; Scalmani, G.; Barone, V.; Petersson, G.A.; Nakatsuji, H.; Li, X.; Caricato, M.; Marenich, A.V.; Bloino, J.; Janesko, B.G.; Gomperts, R.; Mennucci, B.; Hratchian, H.P.; Ortiz, J.V.; Izmaylov, A.F.; Sonnenberg, J.L.; Williams-Young, D.; Ding, F.; Lipparini, F.; Egidi, F.; Goings, J.; Peng, B.; Petrone, A.; Henderson, T.; Ranasinghe, D.; Zakrzewski, V.G.; Gao, J.; Rega, N.; Zheng, G.; Liang, W.; Hada, M.; Ehara, M.; Toyota, K.; Fukuda, R.; Hasegawa, J.; Ishida, M.; Nakajima, T.; Honda, Y.; Kitao, O.; Nakai, H.; Vreven, T.; Throssell, K.; Montgomery, J.A., Jr.; Peralta, J.E.; Ogliaro, F.; Bearpark, M.J.; Heyd, J.J.; Brothers, E.N.; Kudin, K.N.; Staroverov, V.N.; Keith, T.A.; Kobayashi, R.; Normand, J.; Ragahavachari, K.; Rendell, A.P.; Burant, J.C.; Iyengar, S.S.; Tomasi, J.; Cossi, M.; Millam, J.M.; Klene, M.; Adamo, C.; Cammi, R.; Ochterski, J.W.; Martin, R.L.; Morokuma, K.; Farkas, O.; Foresman, J.B.; Fox, D.J.; Gaussian, Inc.: Wallingford, CT, USA, 2016.
41. Adamo, C.; Barone, V. Toward Reliable Density Functional Methods without Adjustable Parameters: The PBE0 Model. *J. Chem. Phys.* **1999**, *110*, 6158–6170. [[CrossRef](#)]
42. Weigend, F.; Ahlrichs, R. Balanced Basis Sets of Split Valence, Triple Zeta Valence and Quadruple Zeta Valence Quality for H to Rn: Design and Assessment of Accuracy. *Phys. Chem. Chem. Phys.* **2005**, *7*, 3297. [[CrossRef](#)] [[PubMed](#)]
43. Grimme, S.; Antony, J.; Ehrlich, S.; Krieg, H. A Consistent and Accurate Ab Initio Parametrization of Density Functional Dispersion Correction (DFT-D) for the 94 Elements H–Pu. *J. Chem. Phys.* **2010**, *132*, 154104. [[CrossRef](#)] [[PubMed](#)]
44. Johnson, E.R.; Becke, A.D. A Post-Hartree-Fock Model of Intermolecular Interactions: Inclusion of Higher-Order Corrections. *J. Chem. Phys.* **2006**, *124*, 174104. [[CrossRef](#)] [[PubMed](#)]
45. Grimme, S.; Ehrlich, S.; Goerigk, L. Effect of the Damping Function in Dispersion Corrected Density Functional Theory. *J. Comput. Chem.* **2011**, *32*, 1456–1465. [[CrossRef](#)]
46. Becke, A.D.; Johnson, E.R. A Density-Functional Model of the Dispersion Interaction. *J. Chem. Phys.* **2005**, *123*, 154101. [[CrossRef](#)]
47. Zvereva, E.E.; Grimme, S.; Katsyuba, S.A.; Burganov, T.I.; Zagidullin, A.A.; Milyukov, V.A.; Sinyashin, O.G. Application of Time-Dependent Density Functional Theory and Optical Spectroscopy toward the Rational Design of Novel 3,4,5-Triaryl-1-R-1,2-Diphospholes. *J. Phys. Chem. A* **2013**, *117*, 6827–6834. [[CrossRef](#)]
48. Sheldrick, G.M. A Short History of SHELLX. *Acta Crystallogr. A* **2008**, *64*, 112–122. [[CrossRef](#)]
49. Farrugia, L.J. WinGX and ORTEP for Windows: An Update. *J. Appl. Crystallogr.* **2012**, *45*, 849–854. [[CrossRef](#)]
50. Spek, A.L. PLATON SQUEEZE: A Tool for the Calculation of the Disordered Solvent Contribution to the Calculated Structure Factors. *Acta Crystallogr. C Struct. Chem.* **2015**, *71*, 9–18. [[CrossRef](#)]